NANO LETTERS

2003
Vol. 3, No. 9
1187−1190

A Carbon Nanotube Cross Structure as a Nanoscale Quantum Device

Alireza Nojeh,*,† Gregory W. Lakatos,§ Shu Peng,§ Kyeongjae Cho,§ and R. Fabian W. Pease†

Departments of Electrical Engineering, Applied Physics, and Mechanical Engineering, Stanford University, Stanford, California 94305

Received May 2, 2003; Revised Manuscript Received June 27, 2003

ABSTRACT

Traditional lithographically defined quantum wells in 2D electron gases are often too big (several hundreds of nanometers to a few micrometers) to exhibit single-electron effects at room temperature. Here, a structure is proposed that makes use of the electromechanical properties of single-walled carbon nanotubes to fabricate a quantum well with a width on the order of a few nanometers. As an example, (8, 0) nanotubes are used in the quantum device, and the corresponding electronic structure is calculated.

Introduction. Single-walled carbon nanotubes can be either metallic or semiconducting on the basis of their chiral angle and diameter. It is also known that flattening the cross section of a nanotube from a circular to an elliptical shape can result in a reduction or increase in the band gap of a semiconducting nanotube[1−3] or a band splitting in a metallic nanotube, a property that can be used to create tunnel barriers and isolate a quantum dot along the nanotube axis using AFM (atomic force microscope) manipulation[4]. Here, the mechanical and electronic structures of a nanotube cross[5−7] device are studied, and it is shown that the structure can act as a nanoscale quantum device, exhibiting level quantizations that must be observable at room temperature. Traditionally, quantum dot devices are made using lithography and are usually larger than a few hundred nanometers. Therefore, level separations due to both quantization and Coulomb charging effects are so small that the thermal excitation of electrons at room temperature prevents them from being observed during the measurement of device properties (i.e., $I-V$ characteristics). For room-temperature single-electron operation, one needs to reduce the dot size to a value that can result in level separations significantly larger than kT (∼26 meV). A simple infinite potential well model estimates that the device size should be only a few nanometers for this purpose. However, devices with these sizes are extremely difficult to make even using electron-beam lithography.

Basic Idea. A single-walled carbon nanotube is a quantum wire where carriers are strongly confined to a nanometer-size region in the two axially transverse directions, making transport through the nanotube essentially 1D. This quantum wire can be turned into a quantum dot if only a confinement in the third dimension is imposed on it, which is much easier than making a dot in bulk material. The question of determining how the required longitudinal confinement can be created along the nanotube axis now remains. This problem can be approached in simple geometrical terms: how can we select a point on a line? A simple answer is to cross the line with a second line (i.e., another 1D object, which, we suggest, could be another nanotube in our structure).

Simulations and Results. If two nanotubes cross, then one can expect mechanical deformation in both at the intersection point. To determine the shape of the structure, we relaxed two (8, 0) nanotubes in a cross junction with Tersoff−Brenner potentials,[8−10] using a single fixed layer of graphite as the substrate. Initial atomic coordinates for the nanotubes were generated using Fortran programs presented by Saito et al.[11] The final relaxed structure (Figure 1) compares very well with an AFM image of a nanotube cross structure on silicon dioxide that we have made using a CVD (chemical vapor deposition) process (Figure 1, inset).[12]

The next step is to evaluate the electronic structure changes in the nanotubes along the axes. Band gap variations as a result of flattening the cross section in an infinitely long and uniform (8, 0) nanotube have been calculated previously using density functional theory (Figure 2).[1] As we start pressing on the tube and changing its cross section to elliptical, the conduction band starts to move down, reducing the band gap, while the states in the valence band remain unchanged. This continues until the point where the index of flattening (defined in the Figure 2 caption) reaches 0.25, where the conduction band edge meets the valence band edge

* Corresponding author. E-mail: anojeh@stanford.edu.
† Department of Electrical Engineering.
§ Department of Mechanical Engineering.

10.1021/nl034278b CCC: $25.00
Published on Web 07/25/2003

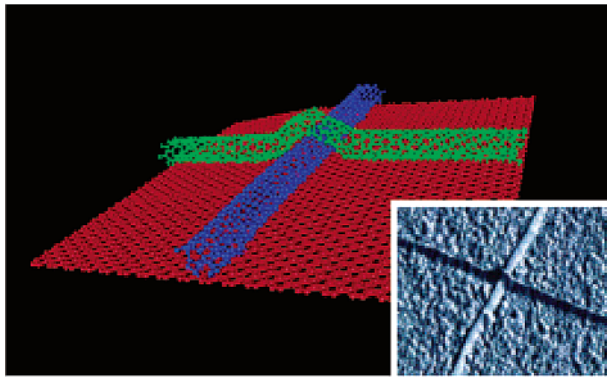

Figure 1. Two crossing (8, 0) single-walled nanotubes on a graphene plane. The mechanical structure was determined numerically using Tersoff−Brenner molecular dynamics. Twenty unit cells of each nanotube are shown in the image. Inset: AFM image of two crossing nanotubes on a silicon dioxide substrate. The nanotubes were grown using a CVD process.

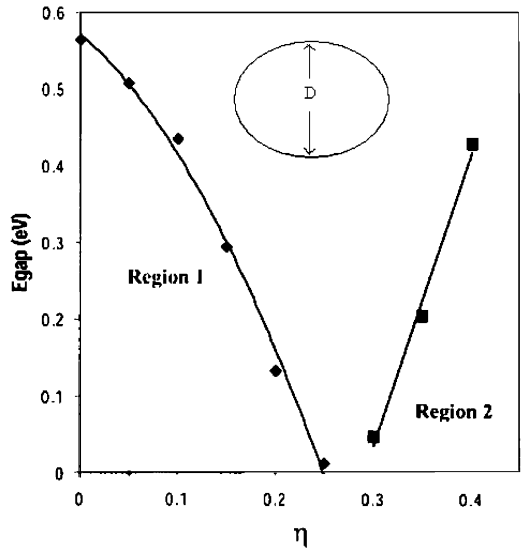

Figure 2. Band gap vs index of flattening in an (8, 0) nanotube, calculated using density functional theory.[1] In region 1, the conduction band edge is lowered. In region 2 (after 0.25 flattening), the valence band edge moves down, reopening the band gap. Inset: Elliptical cross section of a flattened nanotube. The index of flattening is defined as $\eta = (d_0 - D)/d_0$ where d_0 is the diameter of the undeformed nanotube and D is shown.

(the two bands cross), and the nanotube becomes metallic (zero band gap). This all corresponds to region 1 in Figure 2. Beyond this point, if we further flatten the nanotube, DFT calculations show that the conduction band remains constant, and this time, the valence band moves down as a result of more flattening, which is the reason for the reopening of the gap in this region (region 2 in Figure 2).

In the next step, the index of flattening along the top nanotube of Figure 1 is calculated as a function of distance along its axis, and using the curve in Figure 2, the local conduction band edge is estimated. A quantum dot of width ~1.5 nm and depth ~0.3 eV is obtained in the conduction band of this nanotube at the intersection point (Figure 3). Note that in all of the areas where the index of flattening is more than 0.25 the conduction band edge is constant.

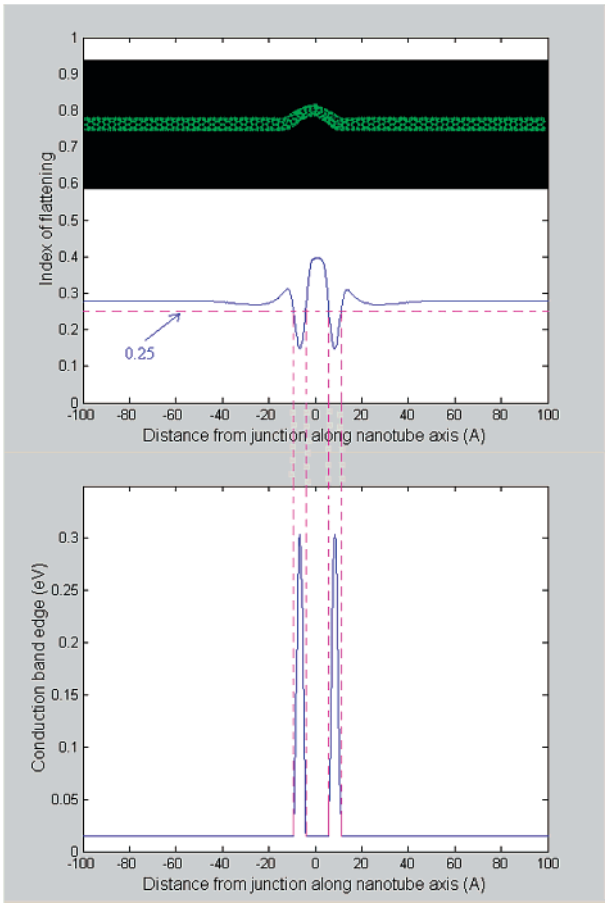

Figure 3. Side view of the top nanotube from Figure 1. The index of flattening (η) is calculated as a function of position along the nanotube axis. Conduction band edge behavior along the tube axis is estimated using the data in Figure 2. In those regions with a flattening of more than 0.25, the conduction band edge is constant (corresponding to region 2 in Figure 2).

However, because the system in Figure 1 is a collection of a limited number of atoms as opposed to a periodic structure, it is more appropriate to explain its behavior in terms of electronic orbitals. Here, a Harrison universal tight-binding scheme[13] is used to determine the energy eigenstates of the system. The local occupation probabilities of states are plotted at two different points along the nanotube axis (Figure 4). In the long undeformed wing of the nanotube, the occupation probability in the energy region around the highest occupied molecular orbital (HOMO) and lowest unoccupied molecular orbital (LUMO) shows a gap (Figure 4a). In the middle of the nanotube (intersection point), the occupation probability of states around the HOMO and LUMO increases, and the gap disappears (Figure 4b).

To provide a better visualization of the band edge variations along the nanotube axis, we need to relate the local state occupation probabilities to the local band edges. We have used the following method: At each point along the nanotube axis, the mean value and standard deviation of the energy within each part (occupied or empty) of the spectrum are calculated, according to the state occupation probability distribution functions such as the ones shown in Figure 4. The local conduction band edge is defined as the mean value

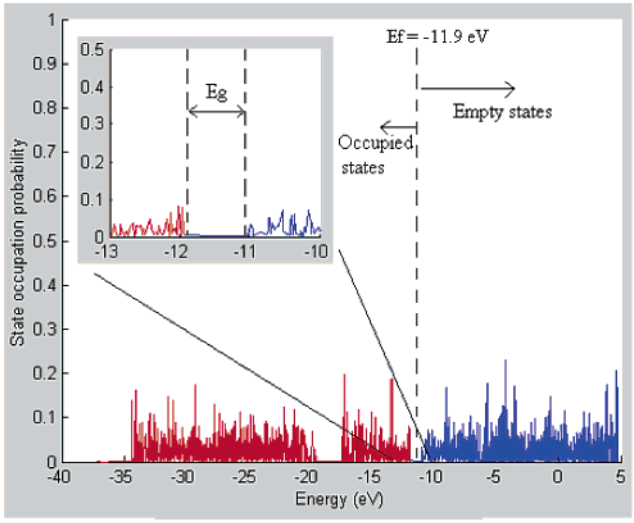

a)

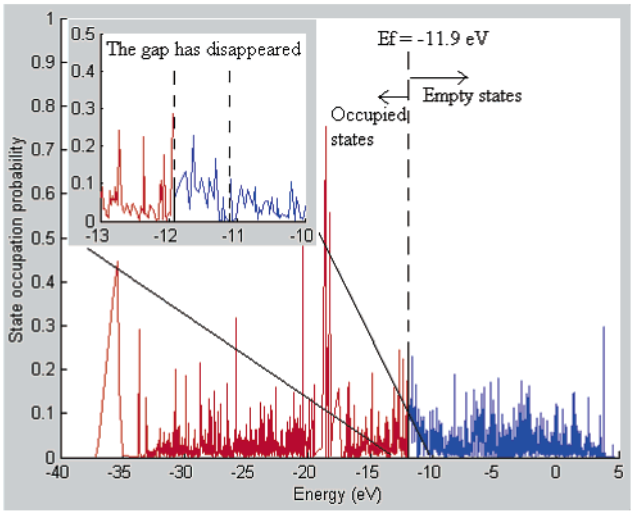

b)

Figure 4. Local state occupation probabilities at two different points along the nanotube axis (for the top nanotube in Figure 1). Harrison universal tight-binding has been used to find the eigenstates of the system. Energy values are relative to free space. (a) At a point in the long undeformed wing of the nanotube, a gap can be seen. (b) In the middle of the tube (intersection point), the gap has disappeared. Insets: Details of the region around HOMO and LUMO.

minus the standard deviation of the energy for the empty part of the distribution function at that point along the nanotube axis. (A similar approach can be used to find the local valence band edge.) Plotting all of the results at different points along the tube axis leads to a curve that is conceptually a sketch of conduction band edge variations with position (Figure 5). Clearly, there is a potential well in the middle of the structure (intersection of the two nanotubes) with a width of about 1.5 nm, reconfirming the simple estimation of Figure 3.

The quantized energy levels for the potential energy function shown in Figure 5 were found using a transmission matrix approach. There are three bound states at −7.78,

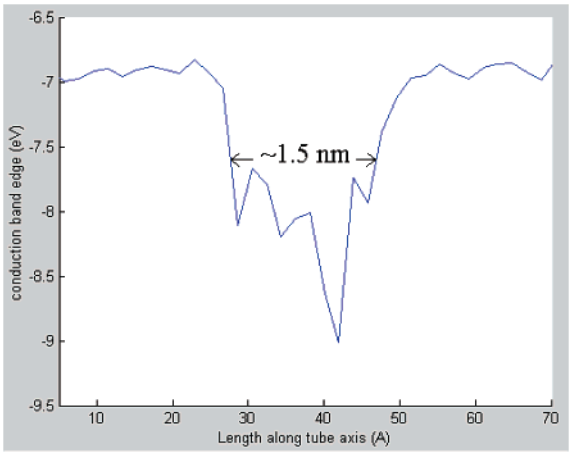

Figure 5. Conduction band edge variations along the nanotube axis for the top nanotube in Figure 1. The band edge at each point along the nanotube axis is defined as the mean value of energy minus the standard deviation in energy at that point. The weight functions used in calculating the mean values and standard deviations are the state occupation probability functions such as those shown in Figure 4.

−7.40, and −7.15 eV in this structure, showing level spacings that are significantly larger than kT at room temperature (26 meV). Therefore, single-electron effects at room temperature should be readily detectable in this structure. Note that so far we are taking into account only the discrete nature of the levels because of quantum confinement. In fact, Coulomb charging pushes the states to even higher energies, making single-electron effects more visible. To estimate the Coulomb charging energies, we can think of our quantum well as a metallic sphere of diameter 1.5 nm as a first-order approximation. For such a sphere, the capacitance is 1.7e−19 F, and the corresponding single-electron charging energy is about 0.5 eV. This amount adds to the state energies, practically leaving only one bound state in the well while shifting the two other levels to higher energies. It should be noted that in the cross structure the bottom nanotube also undergoes mechanical deformation. Our calculations indicate that the amount of flattening all along the bottom nanotube is more than 0.25. Therefore, the band edge behavior is determined by region 2 in Figure 2. A quantum dot for holes in the valence band is created in this nanotube (results not presented here). To explore the effect of the bottom nanotube on the quantum dot in the top nanotube, we repeated the tight-binding calculations of electronic orbitals and band structure in the top nanotube in the presence of the bottom nanotube (rather than as an isolated system). Proximity effects due to the presence of the bottom nanotube led to a slight widening of the quantum dot as well as to a reduction (about 20%) in the depth of the potential well. However, these effects do not jeopardize its functionality as a room-temperature quantum well.

Summary. The relaxed configuration of an (8, 0) nanotube cross structure was found using Tersoff−Brenner molecular dynamics, and the electronic band structure was calculated on the basis of DFT results previously reported for flattened nanotubes. Electronic orbitals were also calculated using a real-space Harrison universal tight-binding method. Both

approaches predict the existence of a quantum well of width ~1.5 nm at the junction point in the top nanotube. Because the separation of energy levels in such a small well is significantly more than the thermal energy at room temperature, these results suggest that room-temperature single-electron effects should be detectable in the transport characteristics of the cross structure. $I-V$ characteristics can be found by calculating the transmission probabilities in the potential functions of Figure 3 or 5 and subsequently using them in a Landauer−Buttiker formalism.[14] However, a more accurate approach would be based on calculating the transmission probabilities using a nonequilibrium Green's function method. We are currently pursuing work in this direction.

Acknowledgment. We thank Professor Hongjie Dai of the Stanford chemistry department for providing CVD facilities and Dr. Thomas W. Tombler for assistance with the growth process. This work was supported in part by the U.S. Department of the Air Force under contract no. F33615-00-1-1728.

References

(1) Peng, S.; Cho, K. *Trans. ASME: J. Appl. Mech.* **2002**, *69*, 451.
(2) Mazzoni, M. S. C.; Chacham, H. *Appl. Phys. Lett.* **2000**, *76*, 1561.
(3) Lakatos, G.; Peng, S.; Cho, K. Unpublished work.
(4) Postma, H. W. Ch.; Teepen, T.; Yao, Z.; Grifoni, M.; Dekker, C. *Science* **2001**, *293*, 76.
(5) Fuhrer, M. S.; Nygard, J.; Shih, L.; Forero, M.; Yoon, Y.-G.; Mazzoni, M. S. C.; Choi, H. J.; Ihm, J.; Louie, S. G.; Zettl, A.; McEuen, P. L. *Science* **2000**, *288*, 494.
(6) Rueckes, T.; Kim, K.; Joselevich, E.; Tseng, G. Y.; Cheung, C.-L.; Lieber, C. M. *Science* **2000**, *289*, 94.
(7) Diehl, M. R.; Yaliraki, S. N.; Beckman, R. A.; Barahona, M.; Heath, J. R. *Angew. Chem., Int. Ed.* **2002**, *41*, 353.
(8) Tersoff, J. *Phys. Rev. B* **1989**, *39*, 5566.
(9) Brenner, D. W. *Phys. Rev. B* **1990**, *42*, 9458.
(10) Brenner, D. W.; Shenderova, O. A.; Areshkin, D. A. *Reviews in Computational Chemistry*; VCH Publishers: New York, 1998; p 213.
(11) Saito, R.; Dresselhaus, G.; Dresselhaus, M. S. *Physical Properties of Carbon Nanotubes*; Imperial College Press: London, 1999; p 227.
(12) Kong, J.; Soh, H. T.; Cassell, A. M.; Quate, C. F.; Dai, H. *Nature* **1998**, *395*, 878.
(13) Harrison, W. A. *Elementary Electronic Structure*; World Scientific: Singapore, 1999.
(14) Datta, S. *Electronic Transport in Mesoscopic Systems*; Cambridge University Press: New York, 1995.

NL034278B